

# A 5G beam-steering microstrip array antenna using both-sided microwave integrated circuit technology

Md. Farhad Hossain, Debprosad Das, Md. Azad Hossain

Department of Electronics and Telecommunication Engineering, Chittagong University of Engineering and Technology, Chattogram, Bangladesh

## Article Info

### Article history:

Received Apr 5, 2023

Revised Jul 13, 2023

Accepted Jul 18, 2023

### Keywords:

Array antenna

Beam-steering

Both-sided microwave integrated circuit technology

Quarter wavelength stub

5G sub-6 GHz frequency band

## ABSTRACT

In this paper a beam steering  $2 \times 2$  microstrip array antenna is proposed and simulated for the 5G sub-6 GHz frequency band. The array antenna is designed at the resonant frequency of 3.5 GHz. The antenna has four patches excited by two microstrip lines. Microstrip lines on top of teflon substrate of 0.8 mm height and slot line in the ground plane makes a hybrid junction. The design uses both sided microwave integrated circuit (MIC) to feed signal to the patch elements. This designed array antenna has the beam steering capability of maximum  $-17^\circ$  to  $+17^\circ$  while keeping the side lobe gain below 10 dB. The simulation results show that the array antenna is designed through good input impedance matching. The antenna has a return loss of -43 dB at center frequency 3.5 GHz. The results also show that the array antenna has a high gain of 12.57 dBi and directivity of 25.11 dB. The maximum gain of this antenna is 24.1 dB at  $-17^\circ$  and  $+17^\circ$ . The proposed work is simulated on keysight technologies advanced designed system (ADS).

This is an open access article under the [CC BY-SA](https://creativecommons.org/licenses/by-sa/4.0/) license.



## Corresponding Author:

Md. Azad Hossain

Department of Electronics and Telecommunication Engineering, Chittagong University of Engineering and Technology

Kaptai, Highway Raozan Pahartali Road, Chittagong-4349, Bangladesh

Email: azad@cuet.ac.bd

## 1. INTRODUCTION

In the modern technological world, beam steering antennas are highly sought-after antennas when a communication link must be formed between end users who are not aligned. Beam steering antenna technology is needed for five generation (5G) mobile connectivity as well as other communication systems including satellite and radar systems [1]–[3]. Because of moving traffic is increasing at an exponential rate, fixed direction radiation beam needs to be modified. As a result of the microstrip array's ability to shape the radiation pattern into a desirable shape, array antennas can be used to modify the fixed direction radiation beam. And the radiation beam can be directed in the direction of moving traffic using beam steering antennas [4], [5]. There are two ways to make these types of antennas: manually directing antenna elements in the desired direction or electrically configuring circuits or antenna elements so that the radiated beam tilts [6], [7].

Several previous studies have been conducted on how a radiated beam of microstrip array antennas can be steered. It can be easily achieved by varying the phase of the array's antenna elements. In addition to phase control, amplitude control of radio frequency (RF) signals may also provide beam steering [8]. A defected ground structure that can increase capacitance or inductance and thus influence the antenna's current flow, causing phase variation and beam steering [9]. However, coupled oscillator arrays using a varactor

diode with microstrip line are used to realize beam steering function without a phase shifter [10]. Altering the distance between the dielectric image line (DIL) and the moving reflector plate underneath it is another method to realize beam steering [11], [12]. Though beam steering may be accomplished by assigning a separate phase to each antenna element in an array, they can only direct the radiated beam at specified angles. Additionally, although internal or external circuit configurations might result in beam steering, they can also increase circuit complexity or antenna size [13], [14]. Incorporating a double-sided microwave integrated circuit (MIC) into a microstrip array can minimize circuit complexity while also shrinking antenna size, resulting in improved circuit function and design flexibility. It may also be used with planar array antennas in a variety of ways to achieve several antenna design functions which makes the design easier [15]–[18].

Moreover, when compared to an antenna array, a single element antenna has limited directivity and gain. Because it offers superior gain and directivity than single element antennas, as well as being easier to build, operate, and install, the microstrip array antenna is the most useful in the communication field. They can also be used to create precise radiation patterns that a single element antenna would be unable to achieve. [19]–[22].

In this work, a microstrip array antenna for beam steering functions exploiting MIC applications is presented. The array antenna is intended to be simulated at resonance frequency 3.5 GHz in sub-6 GHz 5G frequency band due to the enormous expanding number of smartphone users and increasing streaming demand. And in the 4G saturated age, it is required to switch generation while making the implementation effective. For efficient implementation of 5G frequency band, immediate frequency band for this is the sub-6 GHz frequency band [23], [24]. The operational concept of the designed beam-steering array antenna is shown in Figure 1.  $\Delta\Phi$  denoted in the figure is the difference in phase between two input signals. The microstrip line-slot stub junction works as a hybrid coupler in this design and provides signals to the right and left side elements with a phase difference.

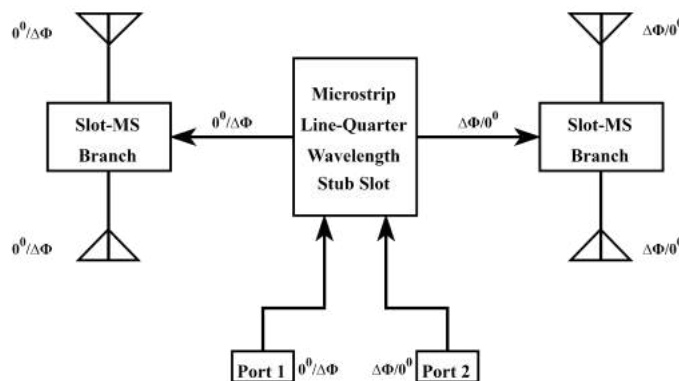


Figure 1. Basic concept of the proposed beam-steering array antenna

The entire simulation is done using keysight technologies advanced design system (ADS) software. Following is the format for the remaining portions of the paper: the design requirements for the suggested antenna are stated in section 3. The simulated outcomes are addressed in section 3, and the conclusion is presented in section 4.

## 2. DESIGN METHOD

This section discusses the proposed antenna architecture, including its feed network and operating principle. The subsection antenna structure describes the antenna's construction. The antenna configuration establishes the feed network with its impedance-matching results, and the array functioning concept is described in the array operating principle.

### 2.1. Antenna architecture

The array antenna presented is composed of four square microstrip patches organized in a  $2 \times 2$  arrangement. Each patch is designed with a resonance frequency of 3.5 GHz. Two quarter wavelength trans-

formers connect the patches on the left and right sides, which are then linked to the source via Magic-T through a slot line by two coupled microstrip lines. Figure 2 shows the geometry of the proposed array antenna with a top view in Figure 2(a) and the cross-sectional view along AA' in Figure 2(b). In the ground plane underneath the substrate layer, a T-type slot line is formed. The patches and microstrip lines are attached to the top layer of a 0.8 mm thick substrate. The relative dielectric constant of the Teflon glass fiber substrate employed in this design is 2.15.

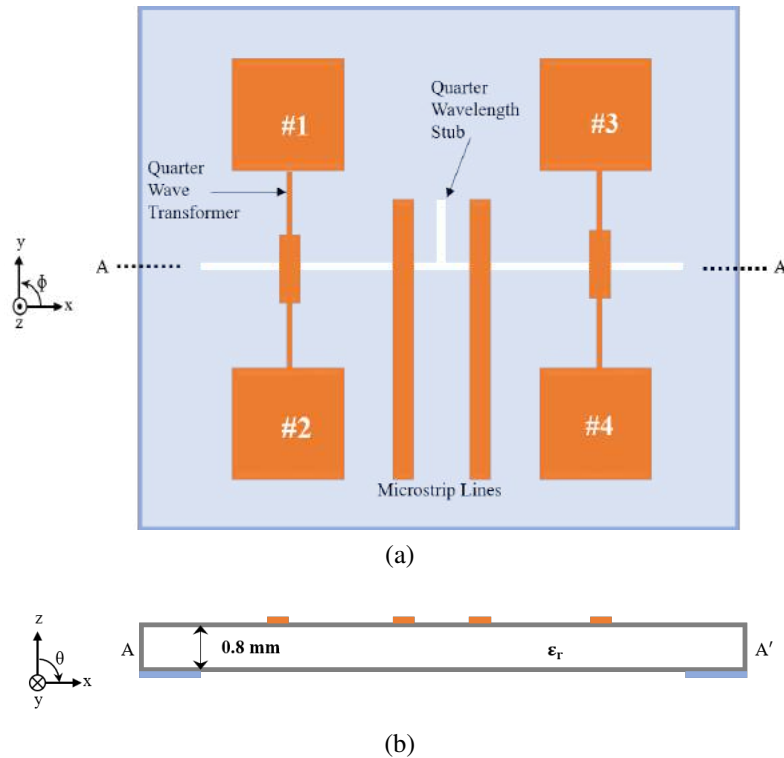


Figure 2. Structure of the proposed beam steering microstrip array antenna (a) top view and (b) cross-section of the antenna along AA'

## 2.2. Antenna configuration

The impedance of the microstrip line is  $50 \Omega$ . The slot impedance must be  $100 \Omega$  in the microstrip-slot branch circuit because it is a parallel power divider. This divider divides the signal into two equal amplitudes in phase signals. The strip impedance must also be  $50 \Omega$  in the slot-microstrip branch circuit as it is a series power divider [25].

This divider divides the signal into two equal amplitudes out of phase signals. For better impedance matching, quarter wave transformers are used which have an impedance of  $92.95 \Omega$  calculated using (1).

$$Z = \sqrt{Z_1 \times Z_2} \quad (1)$$

The slot line at the slot-microstrip branch is extended by a quarter-wavelength for enhanced antenna characteristics, and the quarter-wavelength microstrip line is likewise extended at the microstrip-slot branch. Figure 3 shows the configuration of the proposed array antenna where it can be seen that two slot-microstrip branches are used to link the four antenna elements. Slot-line impedance is twice the microstrip line impedance. Two input ports with  $50 \Omega$  impedance is set to two microstrip lines of width 2.6 mm. Another four ports with each of impedance  $172 \Omega$  are inserted into four quarter wave transformer terminals as shown in Figure 3. Figure 4 shows the frequency response of the array configuration for different values of  $F_d$  where  $F_d$  is the distance between two input microstrip lines. The feed network shows the best impedance matching when the distance between two microstrip lines is 15.2 mm. For  $F_d=15.2$  mm, quarter wave transformer terminal

impedances with respect to input impedance are also shown in Figure 4 and the design parameters are shown in Table 1.

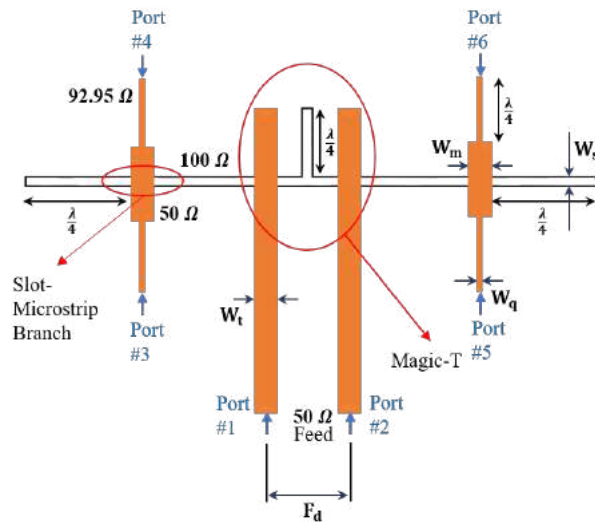


Figure 3. Configurations of the proposed array antenna which contains four radiating square patches, microstrip lines, quarter wave transformers, slot line. Where,  $W_t=W_m=2.6$  mm,  $W_q=0.8$  mm,  $W_s=0.2$  mm,  $F_d=15.2$  mm

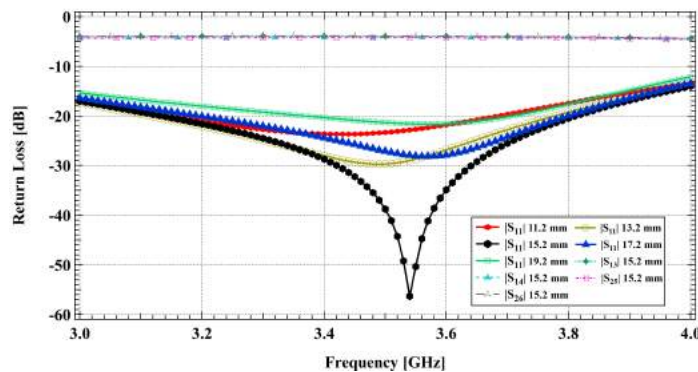


Figure 4. Frequency response of the feed network of the array antenna

Table 1. Antenna design parameters

Parameter	Value	Parameter	Value
Single patch dimension	$30 \times 30 \text{ mm}^2$	Substrate thickness	0.8 mm
Microstrip line width, $w_t=w_m$	2.6 mm	Patch thickness	0.035 mm
Slot-line width, $w_s$	0.2 mm	Relative dielectric constant, $\epsilon_r$	2.15
Substrate material	Teflon glass fiber	Quarter wave transformer width, $w_q$	0.8 mm

### 2.3. Array operating principle

Before moving on to the explanation of the array operating concept, Figure 5 shows how a quarter wavelength stub works when input is only at port #1 in Figure 5(a) when input is only at port #2 in Figure 5(b), and when both ports have simultaneous input signal in Figure 5(c). The quarter wavelength slot of the T-type slot line in the ground plane allows the design to function in a Magic-T fashion.

Magic-T, also known as MIC 180-degree hybrid, is a signal division technique that uses both-sided MIC technology to split a signal into two equal amplitude signals that are in phase or out of phase. The quarter

wavelength slot and two microstrip lines in the design of the proposed array in this paper are built in such a way that if two input signals with a phase difference are fed simultaneously with two microstrip lines and divided in such a way that in phase and out of phase signals propagate through the slot lines, as shown in Figure 5. The schematic electric field distribution is shown in Figures 5(a) and 5(b) when the input signal is fed to ports 1 and 2 separately.

When port 1 receives an input signal, it propagates through the microstrip line and is divided into two equal amplitudes in-phase signals at the microstrip-slot branch, as it is a parallel power divider. The quarter wavelength stub allows the signal to be blocked from propagating to the right side of the slot lines. As a result, port 1 serves as the divider's H port. The signal propagates only to the left side along the slot line. When excited individually, port 2 also acts as an H port of the divider, as shown in Figure 5(b).

The microstrip lines, on the other hand, act as both H and E ports when two ports are excited simultaneously with a phase difference between them. They generate both even and odd component signals as the signal propagates between them and as they are coupled microstrip lines. This orthogonal mode signal is then fed to slot lines, which propagate a sum signal on one side and a difference signal on the other as shown in Figure 5(c).

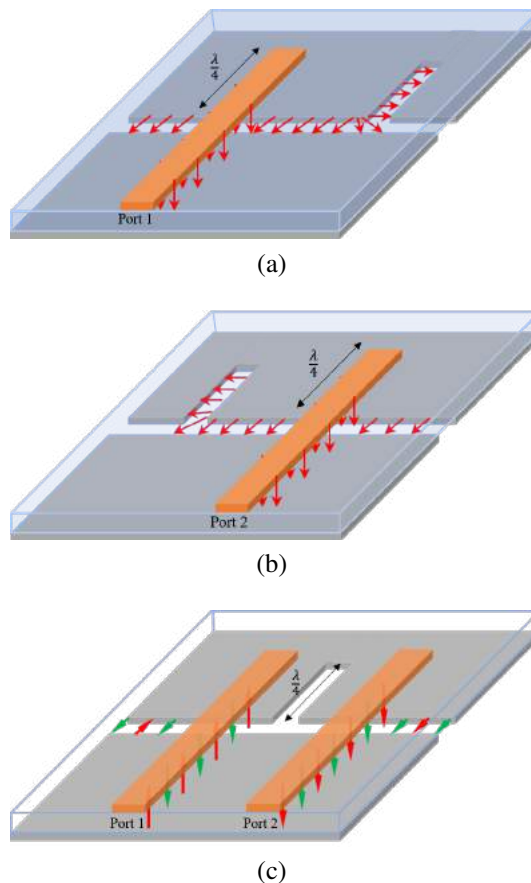


Figure 5. Hybrid coupler structure with schematic electric fields (a) when only port 1 is excited with an RF signal, (b) when only port 2 is excited with an RF signal, and (c) when both ports is excited with RF signals having a phase difference between them

At the microstrip-slot junction of the array, a hybrid coupler is formed by the microstrip feed lines and the T-type slot. The signal propagates on the microstrip coupling line in the orthogonal mode of the common phase component (even mode) and the reverse phase component (odd mode) when two radio frequency (RF) signals are fed to microstrip lines with a phase difference as shown in Figure 6. After that, the hybrid coupler

is used to convert the mode to a slot line. Through a slot-microstrip branch, the signal is then fed to the antenna element. The upper and lower antenna elements are fed with equal amplitude out-of-phase signals because the slot-microstrip branch is a series power divider. So, the antenna elements on the left side and the right side are fed by twice the phase difference of that signal fed at the input point. Thus, the beam steering function is realized.

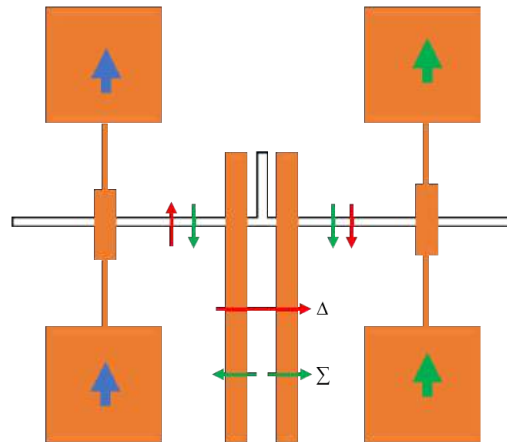


Figure 6. Operation principle of the proposed beam-steering array antenna

### 3. SIMULATED RESULT ANALYSIS

The simulated outcomes and analysis of the results are presented in this section. The following paragraph examines whether the antenna design is impedance matched. The beam steering capability of the antenna is visualized by radiation patterns of the antenna in subsection 3.2. The next subsection describes the design's gain and directivity, followed by a comparison with other existing works.

#### 3.1. Impedance matching and isolation

Figure 7 depicts the reflection coefficient of a beam steering array antenna. It shows the antenna has a return loss of less than -40 dB at a resonant frequency of 3.5 GHz for port 1 and port 2, indicating that impedance matching is good. It is clear from the figure that, 10 dB impedance bandwidth range is from 3.47 to 3.53 GHz though it is a narrow bandwidth antenna but operates at the center frequency of the 5G sub-6 GHz frequency band.

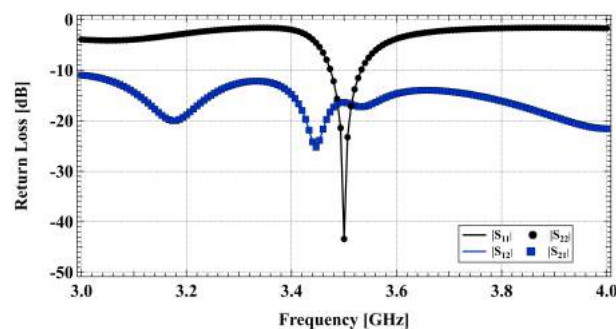


Figure 7. Return loss of the proposed beam-steering array antenna

The antenna also shows good isolation between two input ports. From Figure 7, it is evident that return losses of less than -10 dB are achieved by  $S_{12}$  and  $S_{22}$ , ensuring good port isolation. Hence it can be said that both ports show good impedance matching and better isolation between them.

### 3.2. Radiation pattern

The 3D radiation pattern of the antenna in two cases while feeding the ports is shown in Figures 8 and 9. The pattern for port 2 phase variation is shown in Figure 8. The phase of port 1 has been maintained, while the phase of port 2 is increased by  $15^\circ$ .

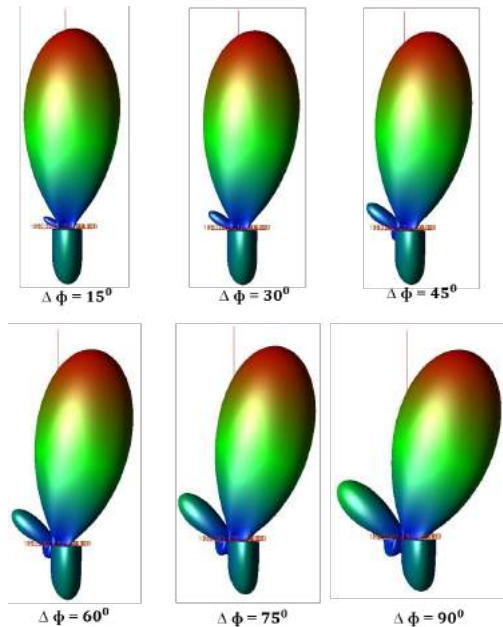


Figure 8. Simulated 3D radiation pattern of the proposed microstrip array antenna, when the phase of the port 2 signal is varied

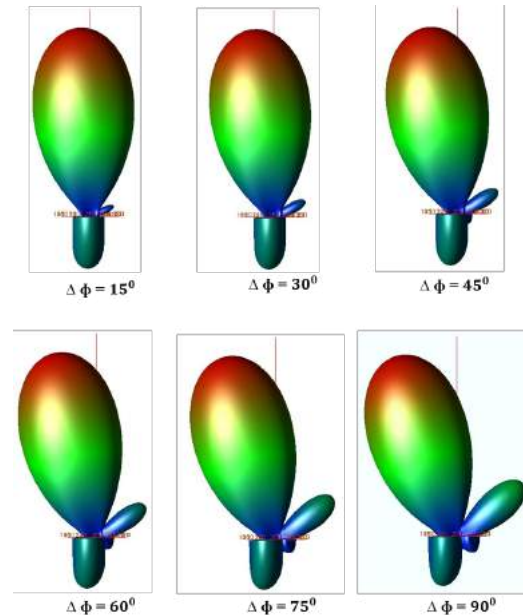


Figure 9. Simulated 3D radiation pattern of the proposed microstrip array antenna, when the phase of port 1 signal is varied

In the second case, the phase of port 1 has been increased by  $15^\circ$  while the phase of port 2 has remained unchanged shown in Figure 9. In both cases, the radiated beam appears to be tilted at a certain angle. The radiated beam tilts in the first case to the opposite direction in the second case, ensuring radiation along the elevation angle, as shown in the figures.

Figures 10 and 11 depicts the 2D radiation pattern for an antenna cut at  $\phi=0^\circ$ . Figure 10 depicts the radiation pattern when port 1 is fed a signal with zero-degree phase variation and port 2 is fed a signal with a certain degree of phase shift. An increment of  $15^\circ$  is used to change the phase of the port 2 signal. The beam tilts  $-17^\circ$  when the phase difference between two ports is  $90^\circ$ . Figure 11 depicts the pattern for a  $15^\circ$ -degree phase shift in port 1, while the port 2 signal has no phase variation. The maximum beam tilt angle in this case is  $+17^\circ$ . In both figures, the blue color pattern represents the pattern for a zero-phase difference between two input signals. The phase difference between two input signals is denoted in the diagram by  $\Delta\Phi$ .

The 2D radiation pattern for a  $90^\circ$ -degree  $\phi$  cut is shown in Figure 12. Because beam steering for this proposed design occurred along an elevation angle, it clearly shows that there is no tilting in the pattern. As a result, when the main beam is tilted, the pattern intensity decreases along the zero degree of the plot for  $\phi=90^\circ$ -degree cut.

### 3.3. Directivity and gain analysis

The proposed antenna's directivity in the  $\phi=0^\circ$ -degree plane and  $\phi=90^\circ$ -degree plane are shown in Figures 13 and 14 respectively. The curve has a shift in the theta axis for the phase difference between two equal amplitude signals fed to ports 1 and 2, but the main lobe directivity remains nearly 25 dB. The curves for the phase difference between ports are shown in Figure 13, where the maximum directivity is at  $-17^\circ$  for a  $90^\circ$ -degree phase difference between two signals when the port 1 signal has a zero-degree phase shift. And has a maximum directivity at  $+17^\circ$  for a  $90^\circ$ -degree phase difference between two input signals when the port 2 signal has a zero-degree phase shift while the port 1 signal's phase is increased at a step of  $15^\circ$ .

From Figure 14, it is visible that the amplitude only decreases along  $\phi = 90^\circ$ , indicating steering of beam only happens along  $\phi = 0^\circ$ .

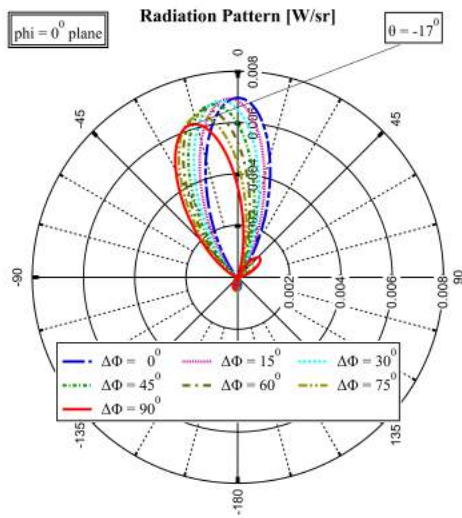


Figure 10. Simulated 2D radiation pattern of the array antenna for  $\phi=0^\circ$  plane, when the phase of port 2 signal is varied

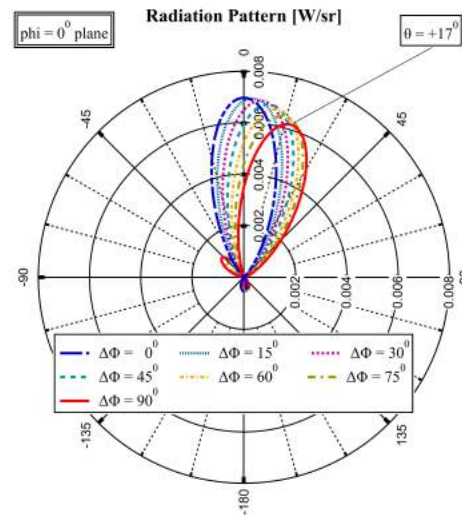


Figure 11. Simulated 2D radiation pattern of the array antenna for  $\phi=0^\circ$  plane, when the phase of port 1 signal is varied

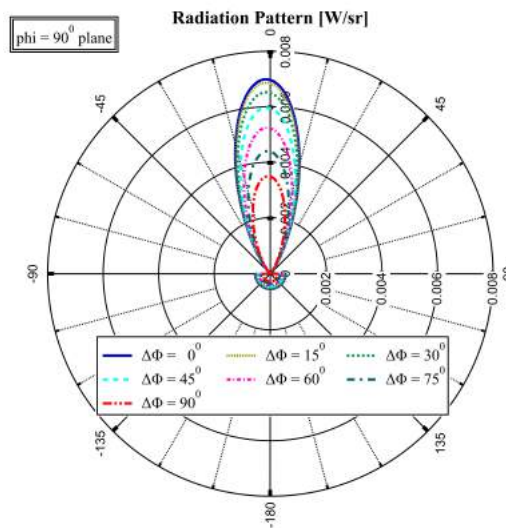


Figure 12. 2D Radiation pattern of the array antenna for  $\phi=90^\circ$  plane

The gain of the proposed antenna array is shown in Figures 15 and 16 for  $\phi=0$  degree and  $\phi=90^\circ$  plane respectively. The main beam can be steered from  $-17^\circ$  to  $+17^\circ$  for a maximum phase difference of  $90^\circ$  between two input signals while keeping the side lobe (SL) gain below 10 dB, as shown in Figure 15.

From Figure 16, it can be seen that all the gain curve has a maximum for several phase difference between two input signals. It confirms that beam steering occurs only in the  $\phi=0$ -degree plane. Figure 17 shows the gain curve in dBi versus frequency. At the resonant frequency of the antenna array, the gain is 12.5786 dBi, as shown in the figure. This means the array antenna has a high gain in the operating frequency.

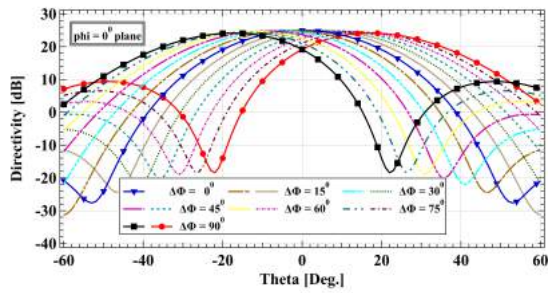


Figure 13. Directivity of the proposed array antenna for  $\phi=0^\circ$  plane

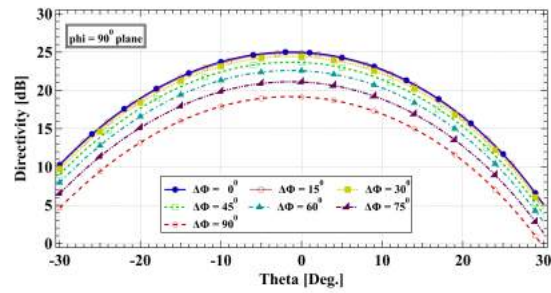


Figure 14. Directivity of the proposed array antenna for  $\phi=90^\circ$  plane

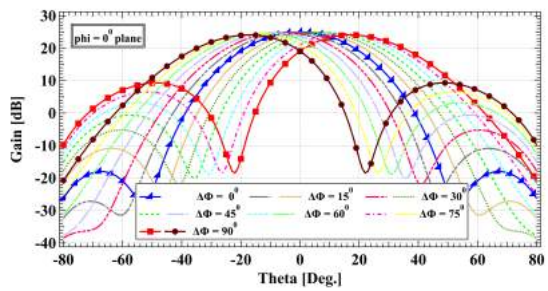


Figure 15. Gain of the proposed array antenna for  $\phi=0^\circ$  plane

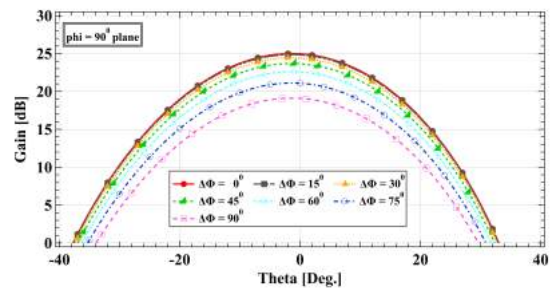


Figure 16. Gain of the proposed array antenna for  $\phi=90^\circ$  plane

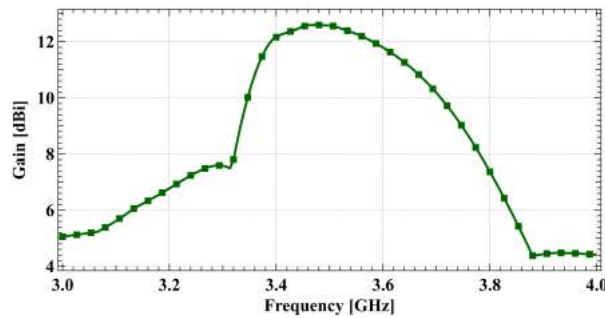


Figure 17. Gain of the array antenna versus frequency

Table 2 shows the overall radiation pattern, which includes gain, directivity, and the maximum angle of beam steering, as determined by the phase difference between two input signals. The proposed array antenna has a gain of about 13 dBi at a resonant frequency of 3.5 GHz, as shown in the table. It is possible to achieve maximum beam steering of  $-17^\circ$  to  $+17^\circ$ .

### 3.4. Comparison with other works

Table 3 presents a comparison of various previous works that use microstrip patches for beam steering. The table clearly shows that this work has the best steering angle among the others. Some of them, among others, use diodes, which require switching operations to operate beam steering and using diodes in an antenna circuit requires biasing, which can compromise antenna performance in terms of impedance matching. Some of them necessitate an external feed circuit, which complicates the design. Despite the fact that one of the

compared works has a greater steer angle than this work, this proposed work outperforms the other antenna parameter by having a high gain and excellent impedance matching performance.

Table 2. Radiation pattern data analysis of the array antenna

$\Phi_1$	$\Phi_2$	Gain (dBi)	Directivity (dBi)	Gain (dB)	SL Gain (dB)	Directivity (dB)	$\Theta_{Max}$
0°	0°	12.5786	12.5786	25.111	-16.729	25.111	0°
0°	15°	12.5688	12.5688	25.089	-10.025	25.089	-3°
0°	30°	12.5381	12.5381	25.023	-4.677	25.023	-6°
0°	45°	12.4809	12.4831	24.903	-0.274	24.903	-9°
0°	60°	12.3827	12.4011	24.704	+2.966	24.741	-11°
0°	75°	12.2526	12.29	24.436	+6.537	24.551	-14°
0°	90°	12.0844	12.1424	24.090	+9.48	24.206	-17°
15°	0°	12.5688	12.5688	25.089	-10.025	25.089	+3°
30°	0°	12.5381	12.5381	25.023	-4.677	25.023	+6°
45°	0°	12.4809	12.4831	24.903	-0.274	24.903	+9°
60°	0°	12.3827	12.4011	24.704	+2.966	24.741	+11°
75°	0°	12.2526	12.29	24.436	+6.537	24.551	+14°
90°	0°	12.0844	12.1424	24.090	+9.48	24.206	+17°

Table 3. Performance comparison of the proposed microstrip array antenna with other works

Reference	Array element no	Gain (dBi)	Return loss	Use of diodes	Max steered angle
[8]	1×2	-	-23 dB	No	27°
[9]	1×2	-	-19 dB	No	15°
[11]	1×8	-	<-10 dB	No	17°
[13]	1×4	6.39	-33 dB	Yes	14°
[14]	1×4	10.98	-27 dB	No	10°
[This work]	2×2	> 12	-43 dB	No	17°

#### 4. CONCLUSION

A beam-steering microstrip array antenna using double-sided MIC technology is designed and simulation results are analyzed in this paper. The proposed array antenna offers high gain and directivity which is about 13 dBi. A beam steering capability of -17° to +17° is achieved by this array antenna. The the antenna has a good input impedance at the center frequency of 3.5 GHz of the sub-6 GHz frequency band which ensures the antennas compatibility to cope with fast-growing mobile traffic and increasing demand for data rate in this present time.

#### REFERENCES

- [1] R. Reese *et al.*, "A millimeter-wave beam-steering lens antenna with reconfigurable aperture using liquid crystal," *IEEE Transactions on Antennas and Propagation*, vol. 67, no. 8, pp. 5313–5324, Aug. 2019, doi: 10.1109/TAP.2019.2918474.
- [2] K. Singh, M. U. Afzal, M. Kovaleva, and K. P. Esselle, "Controlling the most significant grating lobes in two-dimensional beam-steering systems with phase-gradient metasurfaces," *IEEE Transactions on Antennas and Propagation*, vol. 68, no. 3, pp. 1389–1401, Mar. 2020, doi: 10.1109/TAP.2019.2955244.
- [3] J. Yun, D. Park, D. Jang, and K. C. Hwang, "Design of an active beam-steering array with a perforated wide-angle impedance matching layer," *IEEE Transactions on Antennas and Propagation*, vol. 69, no. 9, pp. 6028–6033, Sep. 2021, doi: 10.1109/TAP.2021.3073984.
- [4] K. K. Katare, S. Chandravanshi, A. Biswas, and M. J. Akhtar, "Beam steering architectures for next-generation cellular wireless applications," in *2018 IEEE MTT-S International Microwave and RF Conference (IMaRC)*, Nov. 2018, pp. 1–3, doi: 10.1109/IMaRC.2018.8877180.
- [5] S. K. Sharma, "Design and development of some novel phased arrays and anti-jamming antennas," in *2017 IEEE Radio and Antenna Days of the Indian Ocean (RADIO)*, Sep. 2017, pp. 1–1, doi: 10.23919/RADIO.2017.8242260.
- [6] Q. Zeng, Z. Xue, W. Ren, W. Li, and S. Yang, "Beam-steering lens antenna using two transmit arrays at X-band," in *2019 IEEE Asia-Pacific Microwave Conference (APMC)*, Dec. 2019, pp. 1212–1213, doi: 10.1109/APMC46564.2019.9038766.
- [7] Y. A. Litinskaya, A. D. Nemshon, A. V. Stankovsky, S. V. Polenga, and Y. P. Salomatov, "Experimental research of the antenna array with electronic and combine electronic and mechanical beam steering," in *2016 International Siberian Conference on Control and Communications (SIBCON)*, May 2016, pp. 1–3, doi: 10.1109/SIBCON.2016.7491862.

- [8] S. Mine, E. Nishiyama, and M. Aikawa, "Study on beam controllable antenna by orthogonal excitation," in *International Symposium on Antennas and Propagation*, 2006.
- [9] R. A. Pandhare, P. L. Zade, and M. P. Abegaonkar, "Beam-steering in microstrip patch antenna array using DGS based phase shifters at 5.2 GHz," in *2015 International Conference on Information Processing (ICIP)*, Dec. 2015, pp. 239–243, doi: 10.1109/INFOP.2015.7489386.
- [10] J. Shen and L. W. Pearson, "A design for a two-dimensional coupled oscillator beam-steering antenna array," *IEEE Antennas and Wireless Propagation Letters*, vol. 2, pp. 360–362, 2003, doi: 10.1109/LAWP.2003.822201.
- [11] M.-Y. Li and K. Chang, "Novel low-cost beam-steering techniques using microstrip patch antenna arrays fed by dielectric image lines," *IEEE Transactions on Antennas and Propagation*, vol. 47, no. 3, pp. 453–457, Mar. 1999, doi: 10.1109/8.768779.
- [12] K. Chang, C. T. Rodenbeck, T.-Y. Yun, and M. Li, "Broadband low cost beam-steering techniques for wireless applications," in *IEEE Antennas and Propagation Society International Symposium*, 2002, vol. 2, pp. 496–499, doi: 10.1109/APS.2002.1016130.
- [13] M. Jusoh, M. F. Jamlos, M. R. Kamarudin, M. N. Salimi, F. Malek, and M. I. Jais, "A beam steering patch array antenna for WiMAX application," in *2013 7th European Conference on Antennas and Propagation*, 2013, pp. 924–927.
- [14] C. Liu, S. Xiao, Y.-X. Guo, M.-C. Tang, Y.-Y. Bai, and B.-Z. Wang, "Circularly polarized beam-steering antenna array with butler matrix network," *IEEE Antennas and Wireless Propagation Letters*, vol. 10, pp. 1278–1281, 2011, doi: 10.1109/LAWP.2011.2176903.
- [15] M. Aikawa and H. Ogawa, "Double-sided MICs and their applications," *IEEE Transactions on Microwave Theory and Techniques*, vol. 37, no. 2, pp. 406–413, 1989, doi: 10.1109/22.20068.
- [16] M. Aikawa and H. Ogawa, "A new MIC magic-T using coupled slot lines," *IEEE Transactions on Microwave Theory and Techniques*, vol. 28, no. 6, pp. 523–528, Jun. 1980, doi: 10.1109/TMTT.1980.1130113.
- [17] M. A. Rahman, E. Nishiyama, M. A. Hossain, Q. D. Hossain, and I. Toyoda, "A circularly polarized array antenna with inclined patches using both-sided MIC technology," *IEICE Communications Express*, vol. 6, no. 1, pp. 40–45, 2017, doi: 10.1587/comex.2016XBL0163.
- [18] M. A. Hossain, A. H. Murshed, M. A. Rahman, E. Nishiyama, and I. Toyoda, "A novel dual-band slot-ring array antenna using both-sided MIC technology for polarization detection," *International Journal of RF and Microwave Computer-Aided Engineering*, vol. 32, no. 11, Nov. 2022, doi: 10.1002/mmce.23373.
- [19] J. Ehmouda, Z. Briqech, and A. Amer, "Steered microstrip phased array antennas," *World Academy of Science, Engineering and Technology*, vol. 37, pp. 319–323, 2009.
- [20] S. Mingle, I. Hassoun, and W. Kamali, "Beam-steering in metamaterials enhancing gain of patch array antenna using phase shifters for 5G application," in *IEEE EUROCON 2019 -18<sup>th</sup> International Conference on Smart Technologies*, Jul. 2019, pp. 1–4, doi: 10.1109/EUROCON.2019.8861926.
- [21] K. S. Ahmad, F. C. Seman, and S. A. Hamzah, "Dual microstrip antenna patches with orthogonal I-shaped defected ground structure for beam steering realization," in *2016 IEEE Asia-Pacific Conference on Applied Electromagnetics (APACE)*, 2016, pp. 174–178, doi: 10.1109/APACE.2016.7915880.
- [22] M. A. Rahman, Q. D. Hossain, M. A. Hossain, M. M. Haque, E. Nishiyama, and I. Toyoda, "Design of a dual circular polarization microstrip patch array antenna," in *2014 9<sup>th</sup> International Forum on Strategic Technology*, pp. 187–190, 2014, doi: 10.1109/IFOST.2014.6991101.
- [23] J. G. Andrews *et al.*, "What will 5G be?," in *IEEE Journal on Selected Areas in Communications*, vol. 32, no. 6, pp. 1065–1082, June 2014, doi: 10.1109/JSAC.2014.2328098.
- [24] M. F. Rafdzi, S. Y. Mohamad, A. A. Ruslan, N. F. A. Malek, M. R. Islam, and A. H. A. Hashim, "Study for microstrip patch antenna for 5G networks," in *2020 IEEE Student Conference on Research and Development (SCORED)*, Sep. 2020, pp. 524–528, doi: 10.1109/SCORED50371.2020.9251037.
- [25] K. Egashira, E. Nishiyama, and M. Aikawa, "Planar array antenna using both-sided MIC's feeder circuits," *Electronics and Communications in Japan, Part I: Communications (English translation of Denshi Tsushin Gakkai Ronbunshi)*, vol. 87, no. 7, pp. 23–30, 2004, doi: 10.1002/ecja.10179.

## BIOGRAPHIES OF AUTHORS



**Md. Farhad Hossain**     received the B.Sc. degree in electronics and telecommunication engineering from Chittagong University of Engineering and Technology, Chattogram, Bangladesh in 2018. Currently pursuing an M.Sc. degree in electronics and telecommunication engineering under the supervision of Prof. Dr. Md. Azad Hossain. Presently he is working as a lecturer at the institution. His research interests include antenna design and related readout circuit simulation, experimental analysis, and artificial intelligence. He can be contacted at email: farhad.hossain@cuet.ac.bd.



**Debprosad Das**     Received the B.Sc. degree in electronics and telecommunication engineering from Chittagong University of Engineering and Technology, Chattogram, Bangladesh in 2018. Currently pursuing an M.Sc. degree in electronics and telecommunication engineering under the supervision of Prof. Dr. Md. Azad Hossain. He is currently working as a research assistant at the Department of Electronics and Telecommunication Engineering under Prof. Dr. Md. Azad Hossain. His research interests include antenna design, related circuit simulation, performance analysis, and artificial intelligence. He can be contacted at email: u19mete024p@student.cuet.ac.bd, debudas670@gmail.com.



**Md. Azad Hossain**     (MIEEE) was born in Dhaka, Bangladesh, in 1981. He received his B.Sc. degree in electrical and electronic engineering from Rajshahi University of Engineering and Technology, Rajshahi, Bangladesh, in 2004. The M.Sc. degree in EEE from Saga University, Saga, Japan, in 2010; and the Ph.D. degree in science and advanced technology, in 2013 from the same institute. From 2013 to 2014, he was with Chittagong University of Engineering and Technology as a lecturer. Presently he is working as a professor, head of the Department of ETE at CUET. His research interests include microwave antenna design and related readout circuit simulation and experimental characterization. He can be contacted at email: azad@cuet.ac.bd.